Fall 2017

Analyzing the impact of resolution and aerosol radiation feedbacks on air quality simulation during a winter haze in northern China

Lingyun Du
University of Iowa

ANALYZING THE IMPACT OF RESOLUTION AND AEROSOL RADIATION FEEDBACKS ON AIR QUALITY SIMULATION DURING A WINTER HAZE IN NORTHERN CHINA

by

Lingyun Du

A thesis submitted in partial fulfillment
of the requirements for the Master of Science
degree in Chemical and Biochemical Engineering in the
Graduate College of
The University of Iowa

December 2017

Thesis Supervisor: Professor Gregory Carmichael

Graduate College
The University of Iowa
Iowa City, Iowa

CERTIFICATE OF APPROVAL

_____

MASTER'S THESIS

_____

This is to certify that the Master's thesis of

Lingyun Du

has been approved by the Examining Committee for
the thesis requirement for the Master of Science degree
in Chemical and Biochemical Engineering at the December 2017 graduation.

Thesis Committee: _____
Gregory Carmichael, Thesis Supervisor

_____
Charles Stanier

_____
Jun Wang

ABSTRACT

Winter hazes in East Asia have attracted much attention from researchers. The extremely high concentration of particle matter not only affects people's health, but also has a strong impact on weather and climate. The NASA Unified-Weather Research and Forecasting model (NU-WRF) is a modeling system that can represent aerosol, cloud, precipitation and land processes, and is a great tool to evaluate the aerosol-weather-climate interactions.

To better understand the uncertainties within the model, two applications with different resolutions (45km and 15km) are used for simulations during a haze event in Beijing-Tianjin-Hebei (BTH) area in January 2010. The daily-averaged results of both simulations can estimate the meteorological variables well, with an overestimation in wind speed at 10m. Application with coarser resolution performs better in predicting the temperature at 2m. Hourly-averaged results show that simulation with a coarser resolution does not present obvious diurnal change of meteorology. The rapid change in the simulations for meteorological variables during the "cleaning" stage after the severe haze pollution show a delay in the finer resolution simulation. The simulations of various air pollutants of both resolutions at urban and suburban sites are evaluated. The model performance is not very sensitive to the type of areas, but there are some differences shown between air pollutant species. Simulations of both resolutions can capture the overall trend of $PM_{2.5}$ concentration, but fail to capture the daily peak of PM2.5 in urban/suburban sites, and the $PM_{2.5}$ concentration in the mountain site is overestimated.

During the same haze event, simulations with options related to aerosol direct/indirect feedbacks are compared in this thesis as well. Aerosols have a negative

impact in temperature, water vapor mixing ratio and AOD. The direct feedbacks play the dominant part in decreasing these variables. Both direct and indirect feedbacks have positive forcing at the top of atmosphere. The effect of total feedbacks on the ground is negative, with direct feedbacks having a great negative forcing and indirect feedbacks having a small positive forcing. The meteorological conditions become more stable because of the aerosol radiative feedback. This situation makes it harder for pollutants to disperse, so the $PM_{2.5}$ concentration increase by over 16 μg/m3 in the southern part of BTH area. The aerosol radiative forcing also causes a smaller diurnal variation of $PM_{2.5}$ concentration.

PUBLIC ABSTRACT

Winter hazes in East Asia has attracted much attention from researchers. The extremely high concentration of particle matters not only affects people's health, but also has a strong impact on weather and climate. Aerosol particles in hazes can change meteorology by absorbing and scatter radiation, as well as changing the properties of clouds. It is of much importance to better predict haze and analyze its climate impact.

Chemical transport models are important tools to simulate the meteorology and chemistry in the atmosphere, and the model used in this research is the NU-WRF (NASA Unified-Weather Research and Forecasting) model.

This thesis first discusses the impact of horizontal model resolutions on meteorology and air quality simulations. Results of model applications with two resolutions in urban and suburban sites were compared. The impact of resolutions on predictions can be more obviously shown in diurnal changes than daily changes, whether for meteorological variables or fine particles. Overall the model is not very sensitive to the type of area (urban/suburban), but in the end of the haze event, the time and speed of particle concentration dropping differ between urban and suburban site.

The key characteristic of aerosol in the aerosol-weather-climate interactions, aerosol radiative effect, is also evaluated in the thesis. The aerosol radiative feedbacks tend to cause a more stable meteorological condition during polluted days, and also weakens the diurnal variation of fine particle matter concentration.

TABLE OF CONTENTS

LIST OF TABLES

LIST OF FIGURES

CHAPTER 1 GENERAL INTRODUCTION

1.1 Motivation and Importance of Work

The severe health and climate impacts of air pollution in Asia have attracted much attention from researchers. Associated with many cardiovascular and respiratory diseases, outdoor air pollution was estimated to cause 3.3 million premature death per year worldwide, Asia being the primary contributor of premature mortality (Lelieveld et al., 2015). Additionally, the globally spreading air pollution changes global climate through direct and indirect radiative forcing effects of aerosols.

Haze, defined as an air pollution phenomenon in which low visibility is caused by particulate matter (Chinese National Meteorological Center, 2010), has occurred frequently in recent years in China. During a typical haze period, the concentration of particle matter increases from normal days, the dominant portion of which is fine particles (Cheng et al., 2011; Zhao et al., 2013; Quan et al., 2011). Some researchers evaluated the global distribution of fine particles ($PM_{2.5}$, particles with the diameter less than or equal to 2.5 micrometers) and showed that China, especially eastern China, has a higher $PM_{2.5}$ concentration than most countries and regions (Van Donkelaar et al., 2010).

The winter haze events in the North China Plain (NCP), especially the BTH (Beijing-Tianjin-Hebei) area, have attracted much concern from researchers because of the extremely high aerosol particle concentration. For instance, the BTH area was under a severe haze during 16-21 January 2010. According to the observations conducted by the Chinese Academy of Sciences (CAS) at a downtown Beijing site, the highest daily mean

$PM_{2.5}$ concentration was 260μg/m3, while the 24-hour $PM_{2.5}$ standard in United States is 35μg/m3.

The haze pollution events in BTH area are firstly caused by large anthropogenic emissions. A great amount of primary aerosols and precursors are emitted in this area from industry, traffic and other sources (Zhang el al., 2014; Street et al. 2003), resulting in a high concentration and various species of particulate matters. Moreover, the topography of the BTH area is unfavorable for the pollutants to diffuse. With the Yanshan Mountain in the north and Taihang Mountain in the east, the polluted air is trapped under conditions without northerly winds. The emission factor and meteorological factor combine and interact with each other, resulting in the frequent occurrence of haze in this region.

Chemical transport models (CTMs) are critical tools in analyzing the transport and evolution of various pollutants. To better understand and estimate air pollutions in Asia, many CTMs have been developed and applied under various conditions for years. Despite of the great amount of improvement achieved in air quality modeling, within the models, uncertainties still exist, mainly related to information incompletion/inaccuracy of emissions, initial and boundary conditions, physical and chemical processes and process parameterization (Carmichael et al., 2008). Comparisons between various models, as well as comparisons between different settings within one single model, are critical for the better understanding and applications of CTMs.

1.2 Objectives

This objective of the thesis is to evaluate the simulation of NU-WRF (NASA Unified-Weather Research and Forecasting model) for the winter haze event in the BTH area in January 2010. Two specific objectives are addressed:

1) Analyze the impact of horizontal resolution on meteorological, pollutant and radiation variables and discuss the model performance in urban and suburban areas.

2) Evaluate the effect of direct, indirect and total radiative feedbacks of aerosols in BTH area and better understand the aerosol impact on weather, air quality and climate.

1.3 MICS-Asia Study Overview

It is important to develop a common understanding of the performance and uncertainties of models in Asia applications. A model inter-comparison study which focuses on the long-range transport and deposition of sulfur, i.e., Model Inter-Comparison Study Asia Phase I (MICS-Asia Phase I) (Carmichael et al., 2008), was initiated in 1998 at the international workshop on the transport air pollutants in Asia, and was carried out during the period from 1998 to 2002. A primary aim of that study is to better understand the performance of models source-receptor (S/R) relationships for sulfur deposition. The results from earlier application of regional model for acid deposition in Asia differ significantly between different groups, and MICS-Asia Phase I was intended to help understand the differences and how to model long-range transport in Asia. Eight models participated in this phase of study. The study found that the S/R relationships were most sensitive to uncertainties in the sulfur emission inventory, secondarily to the driving meteorology, and the uncertainties in the model parameters for

wet removal and sulfate production were much less important. MICS-Asia Phase II was initiated in 2003, which was expanded to include nitrogen compounds, O3, and aerosols. Nine different regional modeling groups took part in simulating chemistry and transport of O3, precursors, sulfur dioxide, and secondary aerosols. Four different periods were examined, encompassing two different years and three different seasons. This phase included the global inflow to the study domain, a region-wide database from EANET (the Acid Deposition Monitoring Network in East Asia) observation. The significant differences of predictions between groups were found to be associated with differences in the details of model formulation, parameterizations and numerical methods included.

In 2010, MICS-Asia Phase III was initiated (Gao et al., 2017). This phase of study keeps looking at the inter-comparison of models, and is further expanded. The first topic is to evaluate current air quality models and find out techniques to reduce uncertainties in prediction. The second topic is to develop a reliable emission inventory in Asia. The last topic is to evaluate predictions of aerosol-weather-climate interactions. In the study of Topic 3, the inclusion of online-coupled models to look at the interactions between air quality and climate change makes an important advance of this phase.

MICS-Asia covers a wide range of studies of atmospheric models, including the discussion and comparison within one model. The results in this thesis are part of MICS-Asia Phase III, Topic 3. The simulations with different resolution and aerosol radiative feedback settings of the NU-WRF model will be discussed for a better understanding of the model.

1.4 NU-WRF Overview

The NASA Unified-Weather Research and Forecasting model (NU-WRF) is a modeling system that can represent aerosol, cloud, precipitation and land processes at satellite-resolved scales (roughly 1-25 km). NU-WRF is built upon the Advanced Research WRF (ARW) dynamical core model, and assimilated the NASA earth science observations into the model (C.D. Peters-Lidard et al., 2015).

Six main components are coupled in the NU-WRF system (C.D. Peters-Lidard et al., 2015) as shown in Figure 1.1: the ARW model, the GSFC Land Information System (LIS), the WRF/Chem enabled version of the Goddard Chemistry Aerosols Radiation Transport (GOCART) model, GSFC radiation and microphysics schemes including revised couplings to the aerosols, and the Goddard Satellite Data Simulator Unit (GSDSU).

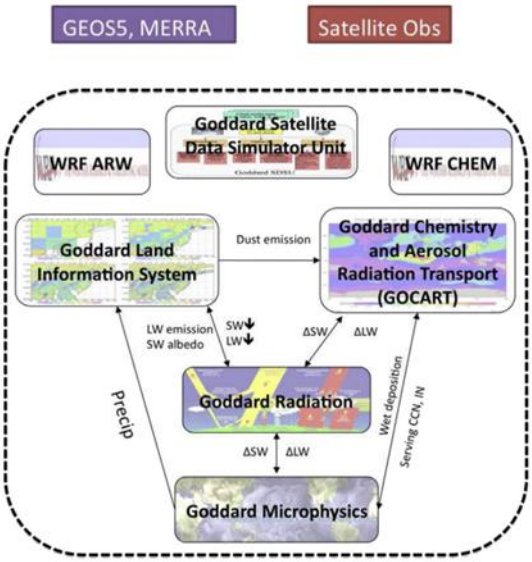

Figure 1.1 A schematic representation of NU-WRF components and their interfaces (C.D. Peters-Lidard et al., 2015)

CHAPTER 2 IMPACT OF SPATIAL RESOLUTION ON AIR POLLUTANT SIMULATION

2.1 Introduction

Spatial resolution, associated with many uncertainties of the CTMs, has an important impact on air quality predicting. The possible factors of the impact are: the spatial resolution of meteorological features which affects transportation, the spatial resolution of emissions, and the spatial resolution where the non-linear chemical reactions occur (Tie et al., 2010).

The impact of resolution on predictions has been addressed and analyzed in many studies. In a simulation of air pollution over a highly industrialized area in China, the results for SO_2, NO, NO_2, CO and PM_{10} showed that the allocation of the emission inventory is improved by applying finer resolution grids, which allows consideration of detailed emission features (Tan et al., 2015). A study over Mexico City focused on ozone and ozone precursors suggests that spatial resolutions, which result from different meteorological condition and transport processes, have larger impacts than that of the resolution associated with emission inventories (Tie et al., 2010). Crippa et al. (2017) found that an enhancement resolution improves model performance for not only meteorological and chemical variables, but also the radiative variables such as aerosol optical depth.

Overall, the use of higher resolution improves the estimation to some extent, it does not always make a better result though. Kuik et al. (2016) found that that a finer

horizontal resolution does not improve the results compared to a coarser resolution with a certain level of detail of the input data (land use classes, emissions).

In this chapter, model results of two resolutions are compared to evaluate if the enhancement of resolution can lead to a better simulation during the northern China winter haze event.

2.2 Methodology and Data

2.2.1 Model description and configuration

Eight models are compared in MICS-Asia Phase III (Gao et al., 2017), two of which (M3 and M4, or D1 and D2 in this chapter) are applications of NU-WRF (two domains with horizontal resolutions of 45km and 15km respectively). The domains of M3 and M4 are shown in Figure 2.1. The module settings for M3 and M4 are listed in Table 2.1.

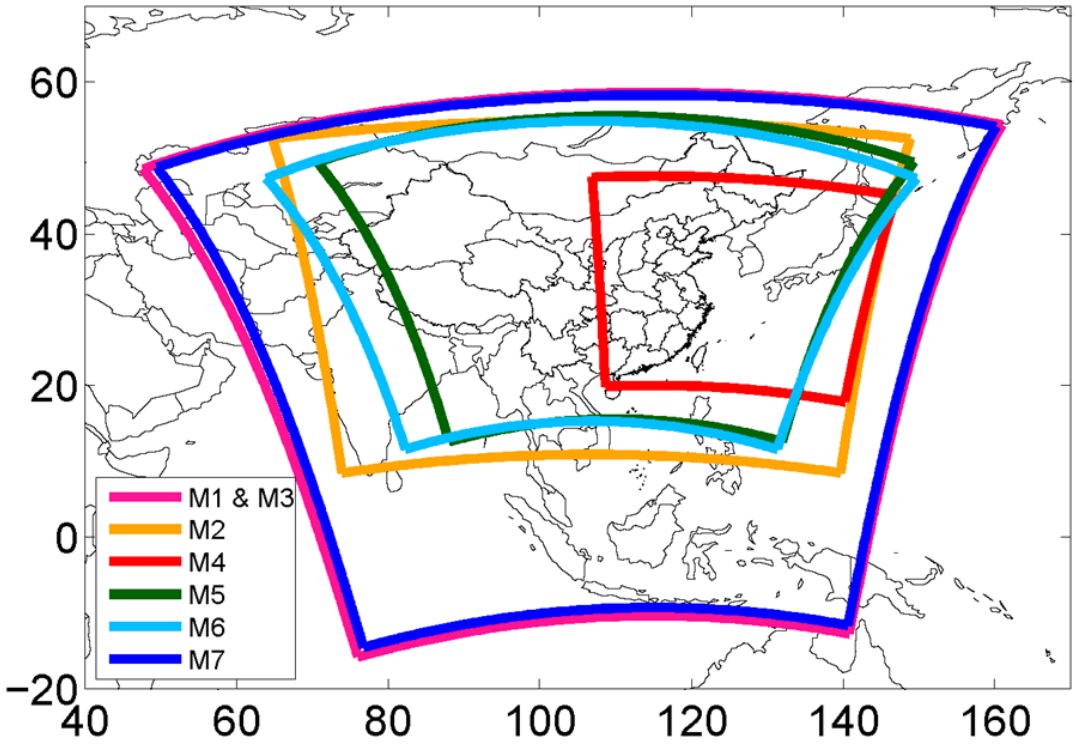

Figure 2.1 The domains of MICS-Asia III (Gao et al., 2017).

Table 2.1 Settings of M3 and M4 (Gao et al., 2017).

Models	M3: NU-WRF1	M4: NU-WRF2
Modelling Group	USRA/NASA	USRA/NASA
Grid Resolution	45km	15km
Vertical Layers	60 layers to 20mb	60 layers to 20mb
Gas phase chemistry	RADM2	RADM2
Aerosols	GOCART	GOCART
Chemical Boundary Conditions	MOZART GOCART	MOZART GOCART

The gas phase and aerosol modules of NU-WRF in this research are the GOCART aerosol model (Chin et al., 2002) coupled with Regional Acid Deposition Model (RADM2) gas phase chemistry. With these modules, the NU-WRF system is capable in simulating various species of aerosols, including sulfate, BC, OC, dust and sea salt.

The emission inventory for this research was developed for MICS-Asia Phase III with state-of the art national/regional inventories (MIX, Li et al., 2017). The boundary conditions are global simulations of atmospheric chemistry (MOZART, Emmons et al., 2010) for gases and GOCART for aerosols. Figure 2.2 shows the MIX emission inventories of January 2010 for various air pollutants.

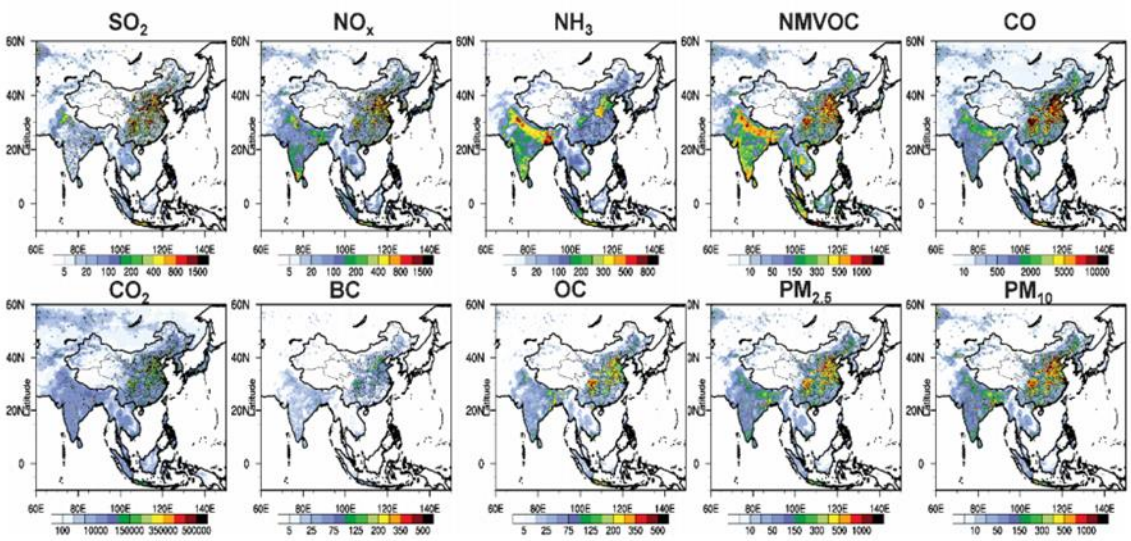

Figure 2.2 MIX emission inventory for January 2010 (Mg/month/grid) (Gao et al., 2017).

2.2.2 Observation data

The operational meteorological measurements (temperature and humidity near surface, wind speed, and downward shortwave radiation), AOD (Aerosol Optical Depth) from Aerosol Robotic Network (AERONET, https://aeronet.gsfc.nasa.gov/) are used. The locations of the meteorological observation sites are plotted in Figure 2.3.

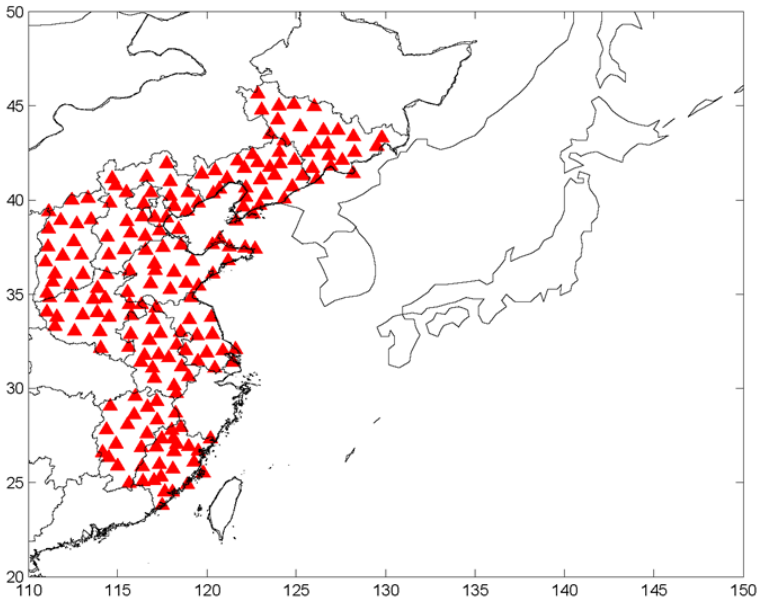

Figure 2.3 Locations of the meteorological observation sites (Gao et al., 2017).

As for air pollutants, the measurement collected from the Campaign on Atmospheric Aerosol Research network of China network (CARE-China) (Xin et al., 2015) are used as well. CARE-China was initially launched by CAS in 2011. Summaries of the CARE-China measurements are listed in Table 2.2. The air pollutant concentration variables include $PM_{2.5}$, PM_{10}, SO_2, NO_2, NO, CO, and O_3.

Table 2.2 CARE-China network sites (Gao et al., 2017).

ID	Site name	Characteristics	Longitude	Latitude
1	Beijing	AOD	116.37	39.97
2	Tianjin	Air quality*	117.21	39.08
3	Shijiazhuang	Air quality	114.53	38.03
4	Xianghe	Air quality	116.96	39.75
5	Xinglong	Air quality	117.58	40.39
6	Beijing Forest	AOD	115.43	39.97
7	Baoding	AOD	115.51	38.87
8	Cangzhou	AOD	116.80	38.28
9	Shenyang	AOD	123.63	41.52
10	Jiaozhou Bay	AOD	120.18	35.90

*Air quality: surface $PM_{2.5}$, PM_{10}, SO_2, NO_x, CO, O_3

For the analysis of urban and suburba n sites in BTH area, the measurements from Institute of Atmospheric Physics (IAP), CAS are used. Hourly averaged concentrations of SO_2, NO_2, NO, and $PM_{2.5}$ were recorded in a few sites around Beijing. The sites at which measurements are used in this research include: Beijing (BJ, urban), Baoding (BD, urban), Shijiazhuang (SJZ, urban), Hengshui (HS, urban), Xianghe (XH, suburban), Cangzhou (CZ, suburban), Zhangjiakou (ZJK, suburban), Lingshan (LS, background). The locations of these sites are shown in Figure 2.4.

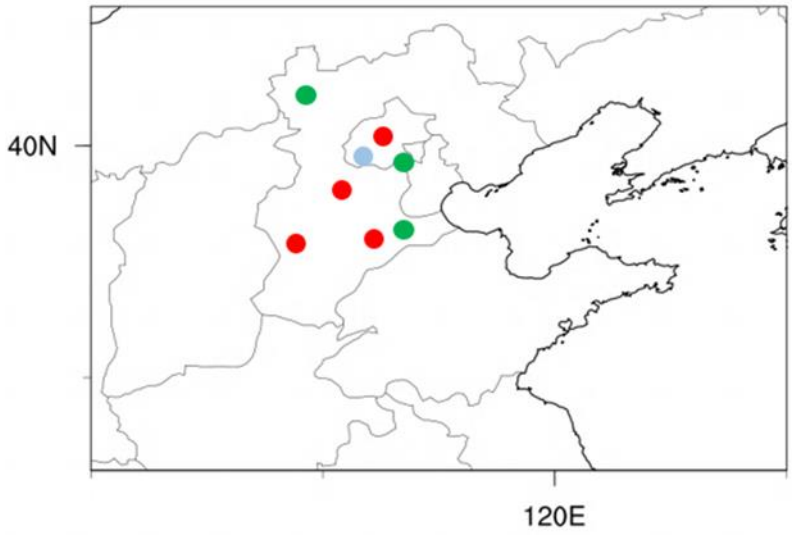

Figure 2.4 Location of the air pollutant observation sites (red dots: urban sites, green dots: suburban sites, blue dot: background site).

2.2.3 Model verification

The performance of M3 and M4 in MICS-Asia III was verified by Gao et al. (2017). The root mean square error (RMSE), mean bias error (MBE), normalized mean bias (NMB), correlation coefficient (r) and other metrics were calculated for the hourly mean meteorological variables at meteorology sites and air pollutant concentrations at the CARE-China sites, presented respectively in Table 2.3 and 2.4.

Table 2.3 Performance statistics of meteorological variables (RMSE and MBE units: degree for T2; g/kg for Q2; m/s for WS10; W/m^2 for SWDOWN (shortwave radiation down)) (Gao et al., 2017).

Metrics	Models	T2	Q2	WS10	SWDOWN South	SWDOWN North
RMSE	M3	2.34	0.16	1.16	60.34	59.56
	M4	2.90	0.43	1.44	100.34	74.89
MBE	M3	-2.18	-0.04	1.11	36.44	47.74
	M4	-2.09	0.11	1.40	26.78	33.59
NMB (%)	M3	-0.79%	-0.34%	9.73%	8.00%	10.63%
	M4	-0.75%	0.95%	12.26%	5.88%	7.48%

Table 2.4 Performance statistics of air pollutants at the CARE-China sites (RMSE and MBE units: ppbv for gases and μm/m^3 for PM (Gao et al., 2017).

Metrics	Models	SO_2	NO_x	O_3	$PM_{2.5}$	PM_{10}		SO_2	NO_x	O_3	$PM_{2.5}$	PM_{10}
r	M1	0.76	0.60	0.46	0.85	0.76	MBE	-17.14	-5.53	-1.54	55.69	30.70
	M2	0.77	0.65	0.48	0.90	0.85		2.10	33.41	2.53	48.44	12.94
	M3	0.69	0.66	0.39	0.85	0.68		-15.89	-8.00	23.93	8.13	-19.92
	M4	0.67	0.61	0.42	0.88	0.73		-9.98	0.28	24.49	23.12	-3.23
	M5	0.72	0.73	0.39	0.91	0.84		-9.69	64.29	-5.30	1.68	-52.49
	M6	0.62	0.48	-	-	-		-27.53	-29.98	-	-	-
	M7	0.57	0.58	0.48	0.82	0.77		-25.56	7.85	-3.09	43.59	-21.00
	Ensemble	0.79	0.71	0.51	0.94	0.87		-14.81	8.90	6.84	30.11	-8.83
RMSE	M1	27.63	33.51	6.40	73.37	79.06	NMB (%)	-14.05	-5.41	7.37	63.57	18.93
	M2	21.00	66.30	8.15	72.44	80.72		12.13	69.58	39.87	54.07	6.38
	M3	29.50	36.87	24.76	47.20	78.21		-10.44	-6.26	306.33	9.67	-12.41
	M4	26.86	36.10	25.34	49.13	72.25		0.31	4.51	316.99	27.03	-1.78
	M5	32.17	87.48	7.90	45.32	81.00		6.83	127.45	-38.49	0.52	-32.94
	M6	33.95	48.62	-	-	-		-51.28	-48.59	-	-	-
	M7	34.75	35.88	6.89	64.25	70.19		-37.87	18.32	-7.78	48.92	-12.78
	Ensemble	24.10	29.12	8.86	45.25	56.65		-13.48	22.80	104.04	33.96	-5.77

2.3 Results and Discussions

In this part, the different performances for the NU-WRF applications with two resolutions are presented and discussed. In January 2010, severe haze occurred in the BTH area. The daily-averaged observations of meteorological variables and fine particle concentration are shown in Figure 2.5. In this research, the discussions focus on one single haze event (16-21 January). On January 16, the concentration of fine particles

increases fast, with a peak of nearly 700μm/m^3 on January 19, followed by a rapid decrease on January 20.

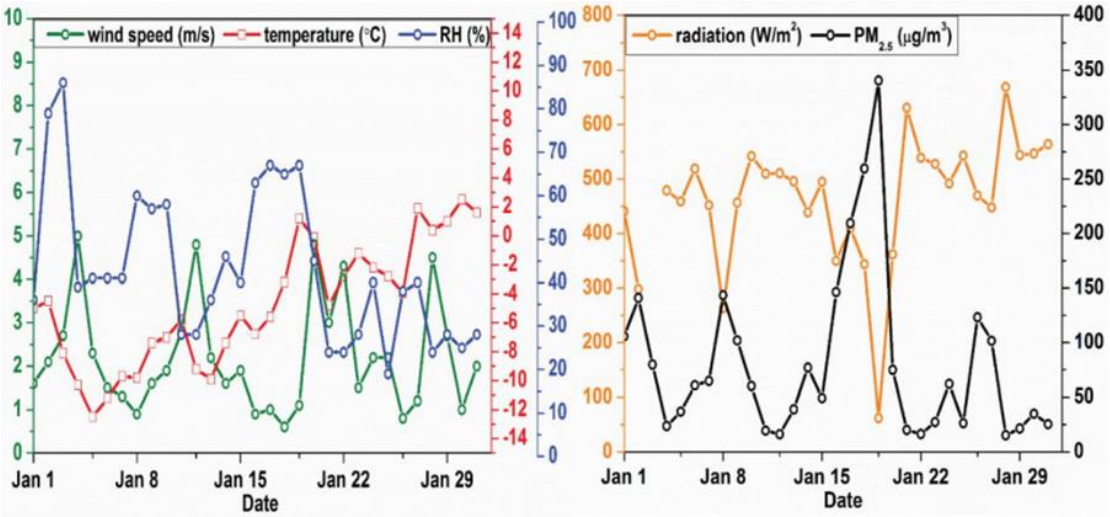

Figure 2.5 Observed near surface daily meteorological variables and PM2.5 concentrations in Beijing for January 2010 (Gao et al., 2017).

2.3.1 Evaluation of meteorological simulation

An important factor that causes winter haze is the stagnant meteorological conditions. According to a previous study (Gao et al., 2016), this haze event had a strong relationship with the meteorological condition in this period. Before the event, the north China plain area was under control of a low pressure system. There has been a weak high pressure system in BTH area from January 16 to January 18, but it was not strong enough to disperse the pollutants and was replaced by a low pressure system afterwards. There was a weak southerly wind from south in BTH area. The severe haze event lasted until January 20, when strong northerly winds carried away the pollutants accumulated during the whole event. For Beijing Site, it can be seen from Figure 2.5 that for January 16-19, the daily-averaged wind speed is lower than 2m/s while the daily-averaged relative

humidity is higher than 60%. From January 19 to 20, the relative humidity decreased for about 20%, and the wind speed increased by more than 3 m/s.

The base cases of M3 and M4 of MICS-Asia III will be named D1 and D2 respectively in the following Chapters. D1 and D2 have horizontal resolutions of 45 km and 15 km. The daily averaged T2 (temperature at 2m), Q2 (water vapor mixing ratio at 2m), and WS10 (wind speed at 10m) in January 2010 at the meteorological sites were calculated and compared with observations. The results are shown in Figure 2.6.

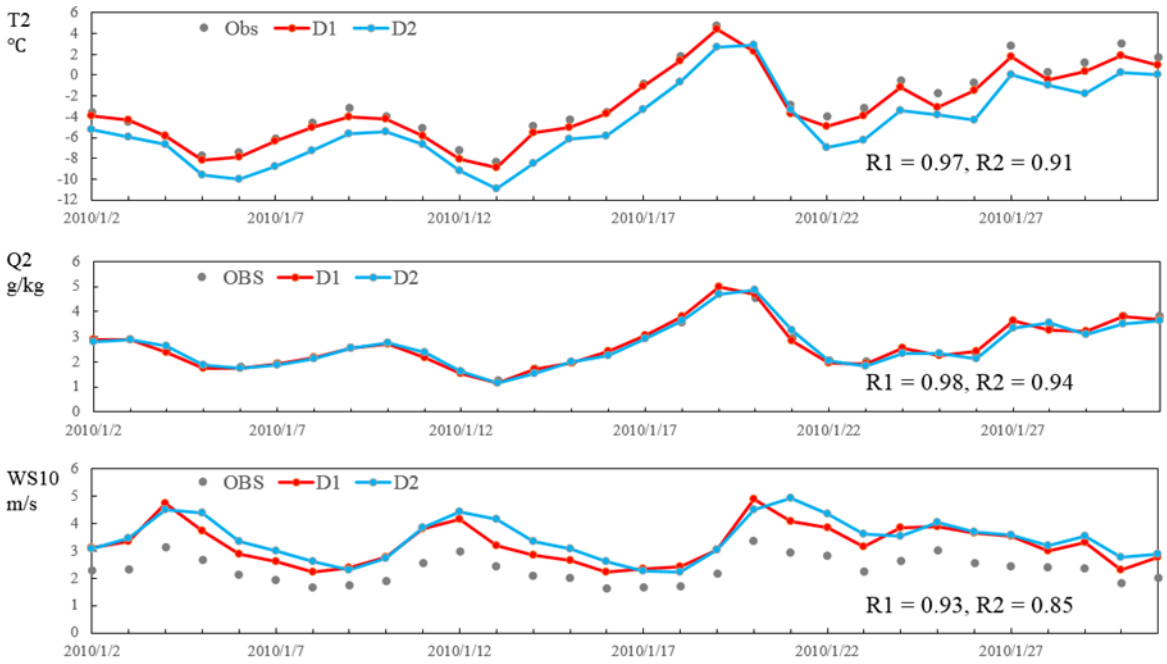

Figure 2.6 Time series of observed (grey) and simulated (red for coarser resolution and blue for finer resolution) daily-averaged 2 m temperature (℃), daily-averaged 2 m water vapor mixing ratio (kg kg $^{-1}$), daily-averaged 10 m wind speed (m s $^{-1}$) at the meteorological sites of MICS-Asia during 2-31 January 2010.

It can be seen from the figure that D1 and D2 both can capture the meteorology well and are in good accordance with each other. As for the temperature, D1 performs better and has a higher correlation coefficient. D2 slightly underestimates T2. The water

vapor mixing ratio in January has been well estimated for both resolutions, and D1 performs better. Both D1 and D2 capture the trend of WS10 and over estimate by around 1 m/s. D2 shows a slower drop of wind speed than the observation on January 20, and has a lower correlation coefficient than D1.

For a better understanding of the different performances between D1 and D2 during the haze event in BTH area, the hourly averaged meteorological variables of Beijing Site during the haze period (January 16-21) were plotted and compared (Figures 2.7 - 2.10).

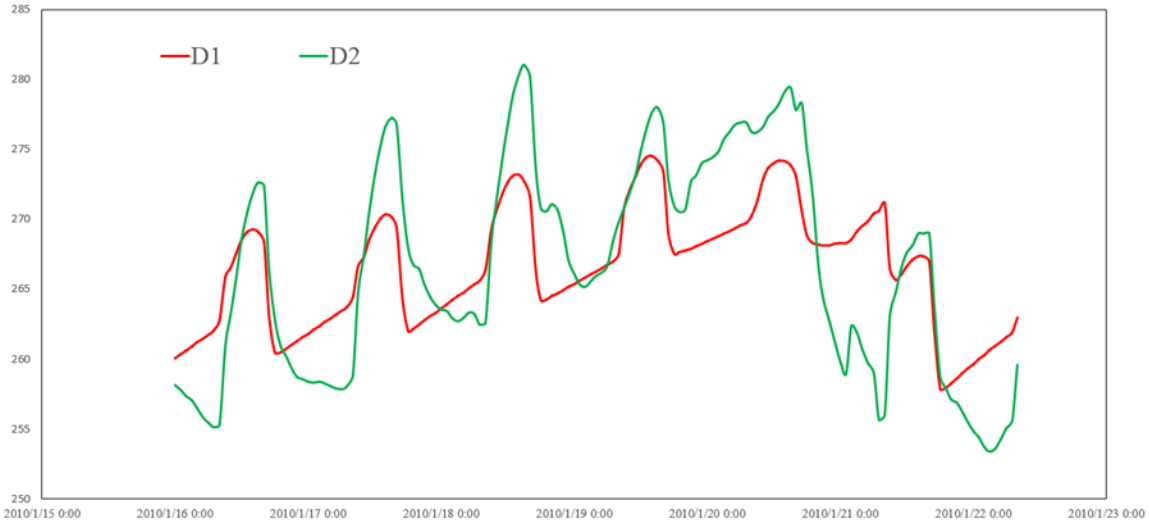

Figure 2.7 The simulated T2 (K) of D1 and D2 at BJ site during the haze event

Figure 2.7 shows the performances of D1 and D2 on T2 simulations. D2 has a greater diurnal difference. It also gives higher values for highest daily temperatures and lower values for lowest daily temperatures.

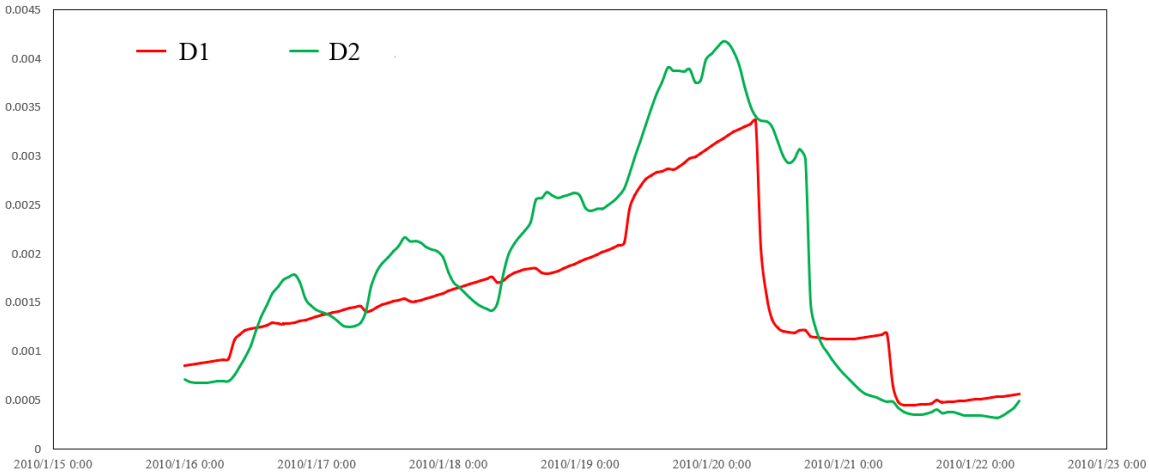

Figure 2.8 The simulated Q2 (g/kg) of D1 and D2 at BJ site during the haze event

In Figure 2.8, the difference between the Q2 simulation of D1 and D2 is presented. There is almost no diurnal variation shown in the results for D1, while D2 shows a clear diurnal change, with the highest mixing ratio in late afternoon and the lowest mixing ratio in the morning. The highest Q2 value in this period for D2 is 0.001 g/kg greater than that of D1. Also, in January 20, the drop of Q2 for D2 shows an 8-hour delay than that of D1.

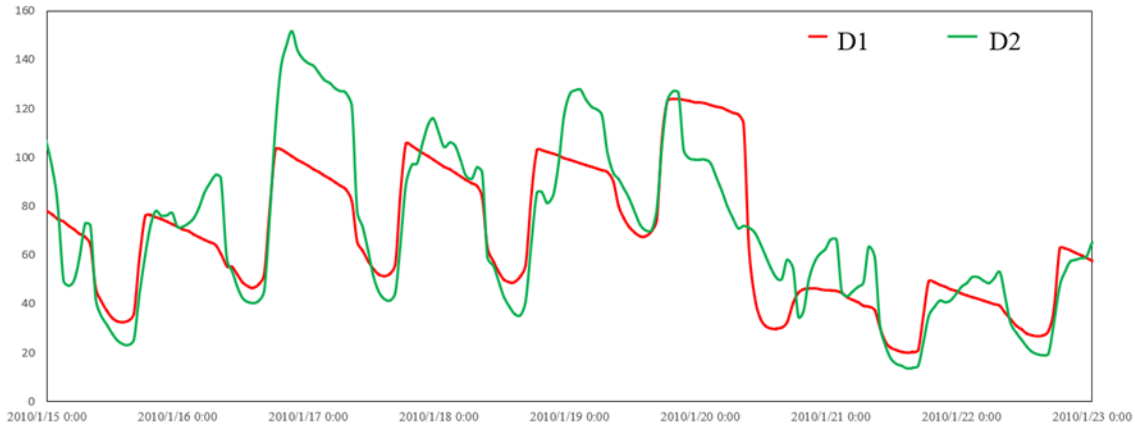

Figure 2.9 The simulated RH2 (%) of D1 and D2 at BJ site during the haze event

Similar time series of relative humidity at 2m (RH2) are plotted in Figure 2.9. Both D1 and D2 show diurnal variation, but D2 captures the peaks in midnight and early morning in January 16-19. The RH2 simulations of D1 and D2 in January 20 are very different: D2 shows a less steep yet earlier drop of RH. The simulations of D1 and D2 after the haze event on January 23 are closer to each other than those during the severe haze.

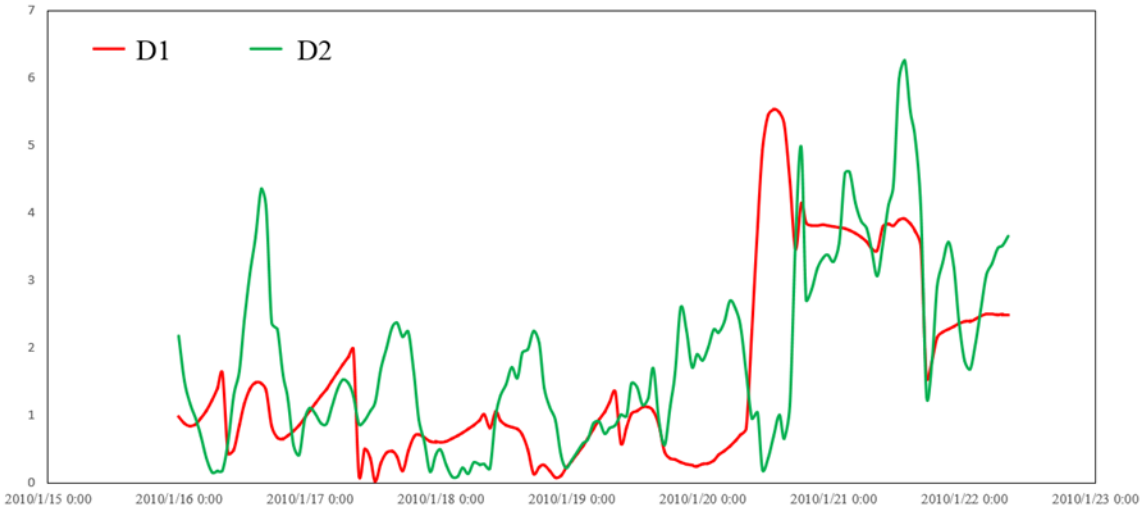

Figure 2.10 The simulated WS10 (m/s) of D1 and D2 at BJ site during the haze event

The wind speed at 10m (WS10) simulation results of D1 and D2 are very different from each other (Figure 2.10). Overall, before January 20, the finer resolution simulation shows a greater diurnal change and the peak value of each day is much greater than that of coarser resolution. In January 20, D1 shows a 6-hour earlier rapid increase of wind speed, and this is in good accordance with its earlier drop in Q2 during the same time period.

Overall, as for the whole January, the daily-averaged results of D1 and D2 simulations can both estimate the meteorological variables well. D2 underestimates T2 a

bit, and both overestimate WS10. When focusing on BJ site, it can be seen that D2 is much more capable in capturing the diurnal change of meteorology. And the rapid change in the simulations for meteorological variables during the "cleaning" stage after the severe haze pollution shows a delay in the result of D2.

2.3.2 Evaluation of air pollutants at various sites in urban and suburban areas

In this part, the hourly-mean measurements of air pollutants (SO_2, NO_2, NO, and $PM_{2.5}$) during January 1-31 at four urban sites: Beijing (BJ), Baoding (BD), Shijiazhuang (SJZ) and Hengshui (HS); 3 suburban sites: Xianghe (XH), Cangzhou (CZ) and Zhangjiakou (ZJK); and 1 background site, Lingshan (LS) are used.

The measurement data and the simulated results of D1 and D2 were analyzed and metrics calculated. The NMBs and NMEs for air pollutants at urban sites for the two resolutions are listed in Table 2.5. Similar comparisons for suburban sites are listed in Table 2.6.

Table 2.5 The NMBs and NMEs for air pollutants at urban sites for the 45km and 15 km resolutions

Pollutants (Urban)	Resolution	NMB(%)	NME(%)
SO_2	45km	-46.6	60.5
	15km	-41.5	60.7
NO	45km	-88.7	93.2
	15km	-89.8	93.1
NO_2	45km	33.6	70.4
	15km	49.5	82.4
$PM_{2.5}$	45km	19.6	53.7
	15km	34.6	57.3

Table 2.6 The NMBs and NMEs for air pollutants at suburban sites for the 45km and 15 km resolutions

Pollutants (Suburban)	Resolution	NMB(%)	NME(%)
SO_2	45km	-1.97	74.7
	15km	-9.39	73.5
NO	45km	-86.6	93.2
	15km	-90.0	93.7
NO_2	45km	11.7	57.8
	15km	-35.7	69.6
$PM_{2.5}$	45km	9.52	60.3
	15km	12.6	63.0

At urban sites, simulations of both resolutions underestimate the concentration of SO2, and the NMB of D2 is slightly smaller than that of D1. The simulations of NO show an underestimation for both resolutions as well, and the NMBs are close to each other. NO_2 is overestimated for both resolutions and D1 performs better. The performance of $PM_{2.5}$ is the best among the four pollutants. D1 gives a smaller NMB and NME in $PM_{2.5}$.

At suburban sites, it can be seen that all the NMBs are smaller than their counterparts at urban sites (except for NO at 15km resolution). Both D1 and D2 underestimate SO_2, but the NMBs are much smaller than in urban sites; the NMEs are about 10% greater, though. The NMBs and NMEs for NO are very close to those of urban sites. The evaluations of NO_2 for both resolutions are better than those of urban sites. Instead of over predicting NO_2 like D1, D2 at suburban sites gives an underestimation. The NME values for $PM_{2.5}$ are even smaller than those of urban sites. It can be seen from the tables that a 15-km resolution simulation does not show much improvement over that of 45-km resolution.

The time series of simulations for urban and suburban sites were also analyzed. The hourly-mean concentration $PM_{2.5}$ at BJ (urban), XH (suburban) and LS (background) sites during January 2-31 are plotted in Figure 2.11.

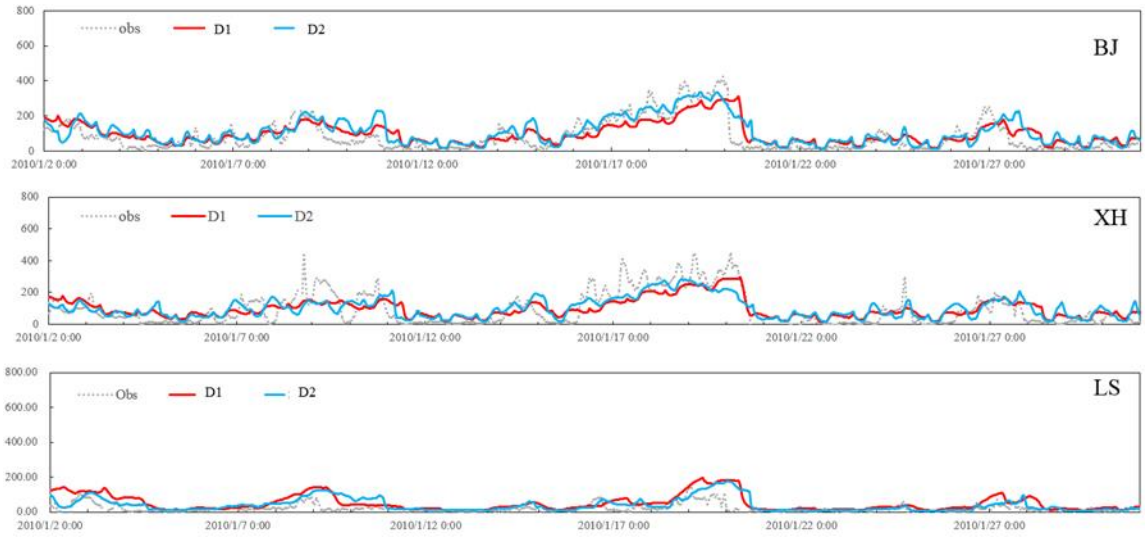

Figure 2.11 Hourly-mean concentration PM2.5 at BJ (urban), XH (suburban) and LS (mountain) sites in January

It can be seen from the figure that both D1 and D2 can capture the overall trend of $PM_{2.5}$. During the most severe polluted period at BJ site, both D1 and D2 underestimate $PM_{2.5}$, and D2 performs better, but neither application captures the daily $PM_{2.5}$ peak. When predicting the $PM_{2.5}$ concentration drop on January 20, the predicted drop of D1 is delayed, while the drop of D2 starts earlier and is less steep than observation. At XH site, both applications underestimate $PM_{2.5}$ and fail to capture the daily peak. The results of D2 are closer to observation from January 16 to 19, but D1 better captures the $PM_{2.5}$ drop on January 20. In the haze event at LS site, D1 and D2 both over estimate $PM_{2.5}$.

2.4 Summary

Overall in January, both D1 and D2 estimate well the meteorological variables. D1 performs better for T2, and both D1 and D2 overestimate WS for about 1m/s. On the other hand, by comparing the hourly averaged results, it can be seen that results of D2 show greater diurnal changes of meteorology.

The performance of predicting air pollutants at urban and suburban sites has been evaluated as well. SO_2 concentrations were underestimated for both resolutions, and D2 performs better. NO was also underestimated for both resolutions, and the results for D1 and D2 are close. Predictions of both resolutions for urban sites and D1 for suburban sites over predict NO2, and D2 for suburban sites under predict NO_2. The performances of $PM_{2.5}$ at suburban sites are slightly better than those at urban sites.

Simulations of both resolutions can capture the overall trend of $PM_{2.5}$ concentration, but fail to capture the daily peak of $PM_{2.5}$ in urban/suburban site, and the $PM_{2.5}$ concentration in the mountain site was overestimated. There are also differences shown in the predictions of the cleaning stage between urban/suburban sites.

CHAPTER 3 IMPACT OF AEROSOL RADIATION FEEDBACKS IN ATMOSPHERIC MODELING

3.1 Introduction

One goal of MICS-Asia III Topic 3 is to understand aerosol-weather-climate interactions. Aerosol not only plays an important role in climate change (Boucher el al., 2013), but also has impacts on meteorology and atmospheric chemistry. This research focuses on the meteorological and chemical effects induced by radiative and microphysics characteristics of aerosol particles. The aerosol radiative and microphysics effects and the following feedback on meteorological/chemical conditions are short-termed (Zhang el al., 2008), which makes them valuable in the better understanding of mesoscale CTMs.

There are different types of aerosol radiative effects. The scattering effect of solar radiation from particles is called the "direct aerosol effect" (Charlson et al., 1992), which results in a cooling surface. The absorption of some strong absorbing particles such as black carbon can cause regional atmospheric heating and thus may reduce the formation of clouds. This effect is called "semi-direct effect" (Twomey, 1974). Some particles have impact on cloud microphysics processes. They serve as cloud condensation nuclei, and changes the cloud properties and optical characteristics of the cloud, which is called the "first indirect effect". The effect on the lifetime of cloud and precipitation is called "second indirect effect".

To evaluate the impact of aerosol feedbacks, online meteorology-chemistry models have been applied (Grell et al., 2011). As for cases of northern China winter haze,

studies of aerosol radiative properties have revealed that fine particles are dominant during the haze events (Yu et al., 2011; Li et al., 2013), and have contributed much of the impacts on meteorology and atmospheric chemistry. Wang et al. (2014) have found that during a haze event in January, 2013, the aerosol-radiation interactions caused great changes in PM2.5 concentration. During the same haze event, Gao et al. (2016) pointed out that the change of PM2.5 concentration induced by feedbacks was caused by the more stable atmosphere.

In this chapter, the NU-WRF results of meteorological, radiation and air pollutant variables during the same haze event as Chapter 2 are analyzed. Three scenarios of simulations are compared to find out the impact of aerosol direct and indirect feedbacks.

3.2 Methodology and Data

The model used in this chapter is NU-WRF with the identical settings with D2 (horizontal resolution of 15 km) in Chapter 2, except for the options related to aerosols in the GOCART module. Three groups of module output are used. The first s (I) is the base scenario and has the ACR (aerosol microphysics and radiation) option on, which means that it has included both the direct and indirect feedbacks. The second group (II) has the ACR option off and lacks all feedbacks. The third group (III) has the AR (aerosol-radiation interaction) on, which means it includes the direct feedbacks but lacks indirect feedbacks. The total (direct + indirect) feedback induced change can be calculated by subtracting II from I. The indirect feedback induced change can be calculated by subtracting III from I. The direct feedback induced change can be calculated by subtracting III from II.

The observation data used in this chapter is the hourly measurements of T2, Q2, WS10, AOD and $PM_{2.5}$ concentration at the Beijing Site during January 2010, as mentioned in Chapter 2.

3.3 Results and Discussions

3.3.1 Aerosol feedback impacts on meteorology and surface radiation during the haze

Results for three scenarios with different settings in aerosol feedbacks for the severe haze period (January 16th to 21st) have been analyzed, showing respectively the conditions for prediction with both kinds of aerosol radiation feedbacks (direct and indirect), with direct feedbacks only, and with no feedbacks. The feedback-induced changes of meteorology and surface radiation variables can then be calculated by subtracting the results of the scenarios lacking any feedbacks from the base scenario with all feedbacks.

The contributions from aerosol radiative feedbacks in the change of temperature at 2 m (T2) are shown in Figure 3.1. During the haze period in Beijing and Hebei area, the indirect aerosol feedbacks led to an increase by about 0.2 to 1 °C, with the direct aerosol feedbacks decreasing T2 by about 2 °C. The two feedbacks add up to an overall cooling effect, with T2 in Beijing and Hebei decreasing around 1.4 °C.

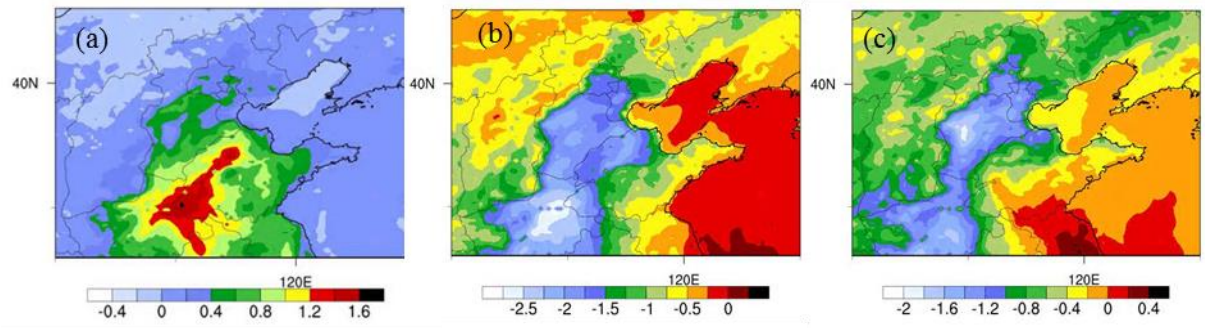

Figure 3.1 The spatial distribution of change in temperature (°C) at 2 m induced by (a) indirect, (b) direct and (c) both direct and indirect aerosol radiative feedback, averaged during Jan 16-21.

Similar analysis has been made for the water vapor mixing ratio at 2 m (Q2) and is shown in Figure 3.2. A slight increase of Q2 of around 0.0001 to 0.0003 kg / kg in Beijing and Hebei is caused by the indirect feedback. And the direct feedbacks caused a decrease of 0.0002 to 0.0004 kg / kg in the area, adding up to a total decrease of 0.0001 to 0.0002 kg / kg.

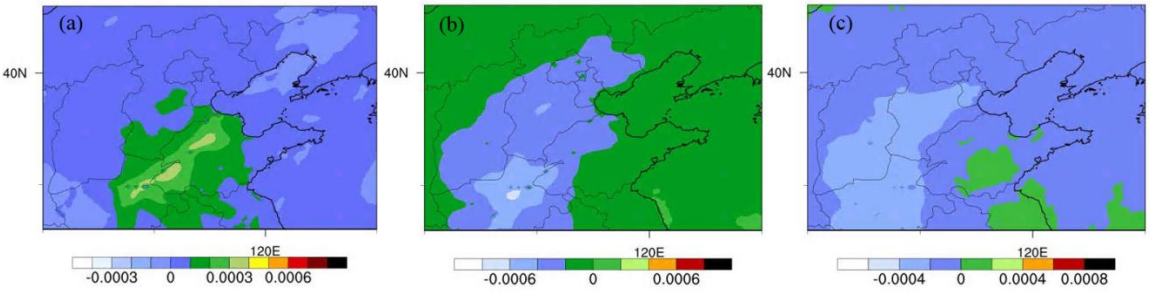

Figure 3.2 The spatial distribution of change in water vapor mixing ratio (kg / kg) at 2 m induced by (a) indirect, (b) direct and (c) both direct and indirect aerosol radiative feedback, averaged during Jan 16-21.

The radiation variable results show the effect of changes in aerosol radiation feedback settings as well, which is shown in Figure 3.3. Figures 3.3 (a) – (c) shows the aerosol feedback impact on AOD 550 (aerosol optical depth at 550 nm). In BTH area, a

decrease of 0.01 to over 0.06 is induced by direct feedback. An increase of 0.01 to over 0.04 in a similar pattern is induced by indirect feedbacks in the same area. The total feedbacks caused a decrease of 0.01 to over 0.04 in BTH.

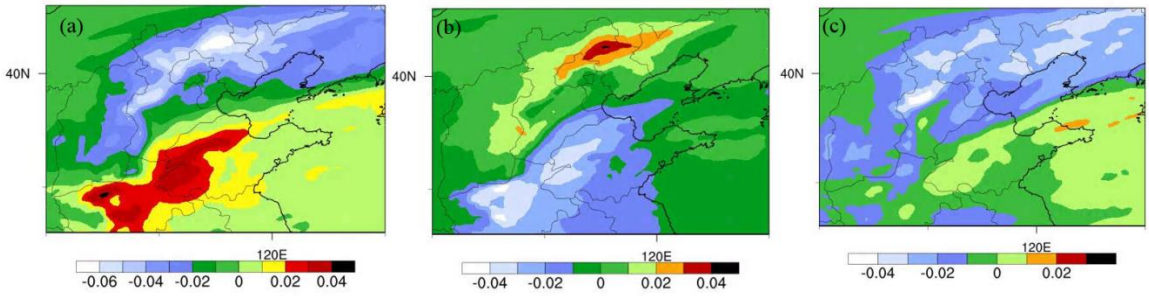

Figure 3.3 The spatial distribution of change in aerosol optical depth at 550 nm induced by (a) direct, (b) indirect and (c) both direct and indirect aerosol radiative feedbacks, averaged during Jan 16-21.

The net radiative forcing (NRadF) was simulated in this research as well. The aerosol induced changes of net radiative forcing at the top of atmosphere (NRadF_TOA) are shown in Figures 3.4 (a) – (c). The direct feedbacks induced an increase up to 20 W/m^2 in most of BTH area, and the indirect feedbacks induced an increase up to 5 W/m^2 in the southeast half of BTH, and a decrease up to 5 W/m^2 in the other half. Overall, the total aerosol induced effect on NRadF_TOA is an increase up to 20 W/m^2 in BTH area, especially the southeastern part.

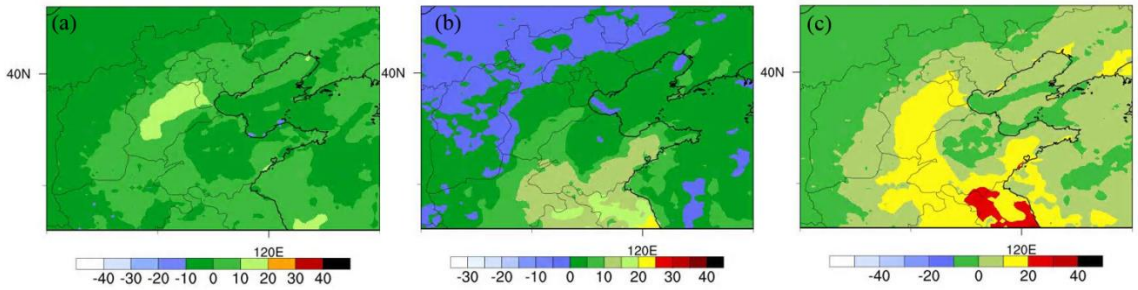

Figure 3.4 The spatial distribution of change in NRadF_TOA (W/m2) induced by (a) direct, (b) indirect and (c) both direct and indirect aerosol radiative feedback, averaged during Jan 16-21.

The aerosol induced changes of net radiative forcing at ground (NRadF_GRD) are presented in Figures 3.5 (a) – (c). The direct feedbacks caused a decrease of 10-20 W/m^2 and the indirect feedbacks caused a -5 to 5 W/m^2 change in the area. The total effect is a decrease up to 20 W/m^2.

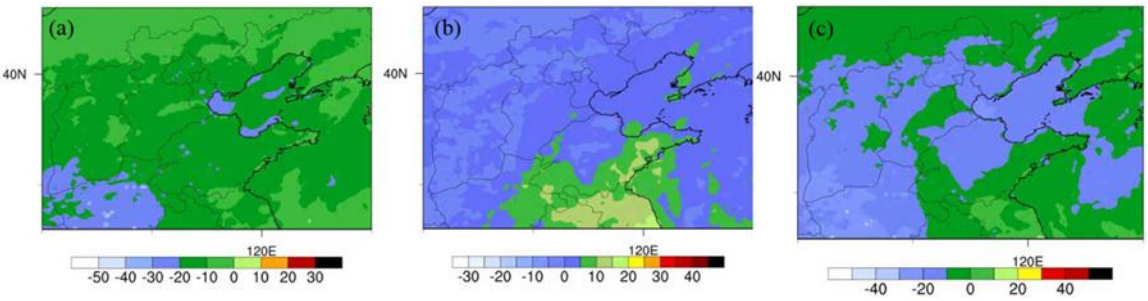

Figure 3.5 The spatial distribution of change in NRadF_GRD (W/m2) induced by (a) direct, (b) indirect and (c) both direct and indirect aerosol radiative feedback, averaged during Jan 16-21.

The subtraction of NRadF_GRD from NRadF_TOA is the net radiative forcing in the atmosphere (NRadF_ATM), which more clearly shows the radiative effect of aerosol feedbacks in the atmosphere. In Figures 3.6 (a) – (c), it can be seen that the direct feedbacks have a strong increasing effect on NRadF_ATM at up to 28 W/m^2 in BTH area.

The effect of indirect feedbacks is not so strong (-2 to 2 W/m^2 in most of BTH). The total aerosol radiative feedbacks lead to an even greater increase of NRadF_ATM.

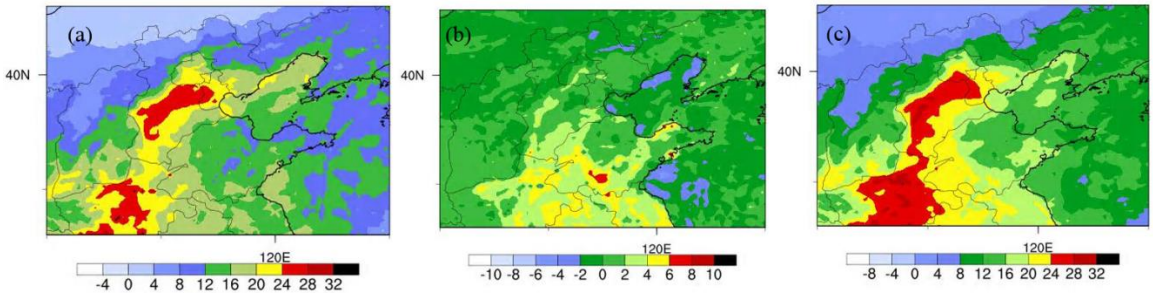

Figure 3.6 The spatial distribution of change in NRadF_ATM (W/m2) induced by (a) direct, (b) indirect and (c) both direct and indirect aerosol radiative feedback, averaged during Jan 16-21.

The time series of aerosol induced changes of meteorological and radiation variables are plotted at Beijing Site for January 2010. Figures 3.7 – 3.13 present respectively the effects for T2, Q2, WS10, AOD, NRadF_TOA, NRadF_GRD and NRadF_ATM.

Figure 3.7 show the time series of aerosol impacts in T2. The effect of aerosol feedbacks is mainly the cooling effect from direct feedbacks for most days in January. However, in the most polluted days, the effect of indirect feedbacks becomes greater, showing a strong cooling effect during the night and strong warming effect during the day.

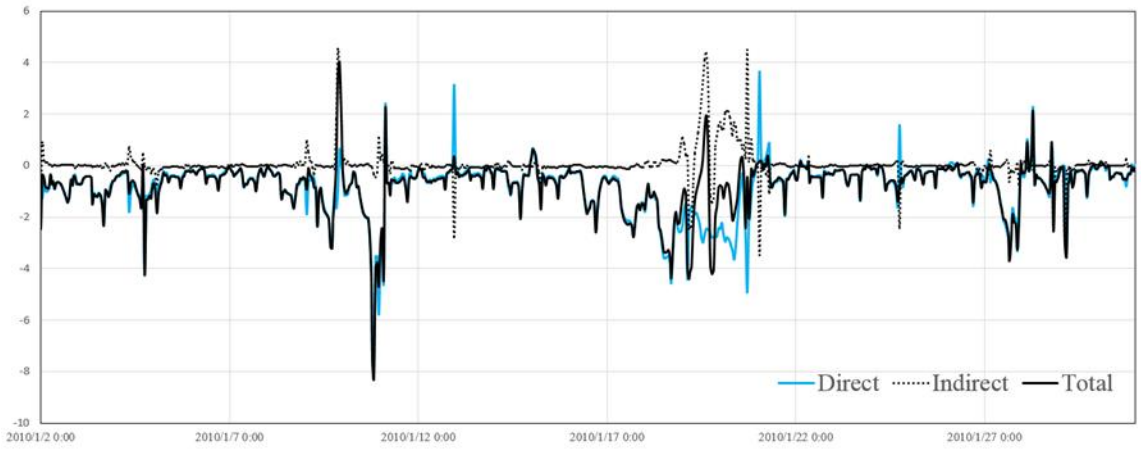

Figure 3.7 Time series of direct, indirect and total aerosol impacts on T2 (°C) during the haze event at BJ site

Similar plots are made for Q2 (Figure 3.8). In the severe polluted days, the indirect feedbacks cause a humidifying effect while the direct feedbacks cause a greater drying effect.

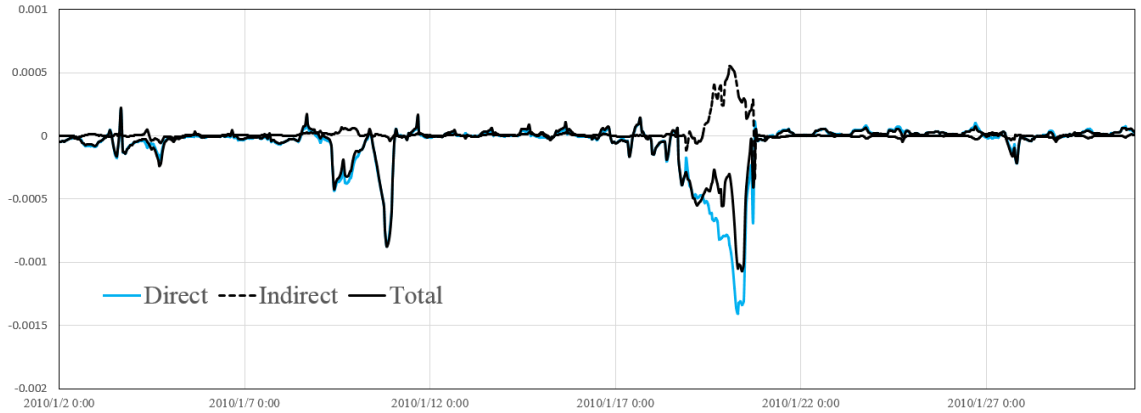

Figure 3.8 Time series of direct, indirect and total aerosol impacts on Q2 (kg / kg) during the haze event at BJ site

The aerosol effect on WS10 vary diurnally, which can be seen in Figure 3.9. The dominant effect is from direct feedback, which is mostly decreasing during the day. In the

severe haze event, both the direct and indirect feedbacks lead to a strong increase in WS10, and the greatest total increase is 2.4 m/s.

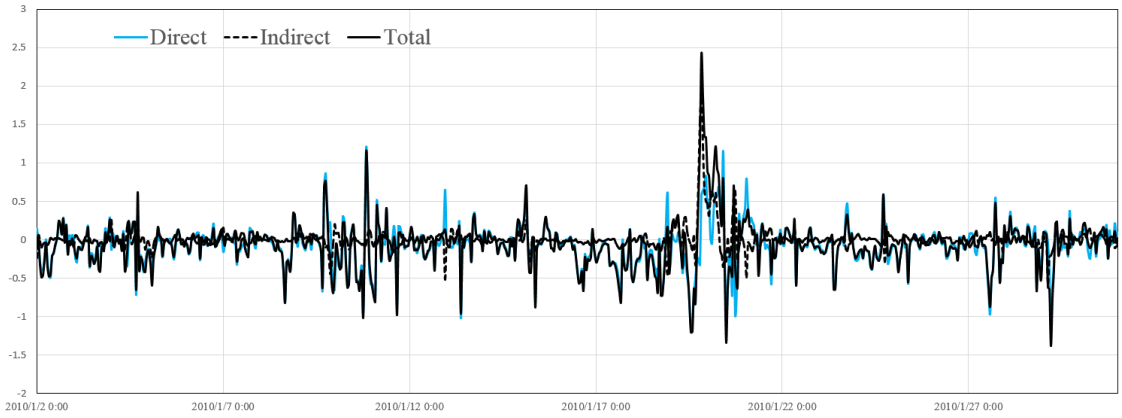

Figure 3.9 Time series of direct, indirect and total aerosol impacts on WS10 (m/s) during the haze event at BJ site

The impacts of both direct and indirect feedbacks on AOD550 are relatively weak during clear days (Figure 3.10). In the haze event, the direct feedbacks have a strong decreasing effect of 0.78 at the greatest, and the increasing effect of indirect feedbacks can be as great as 0.46. The overall aerosol effect on AOD550 is negative.

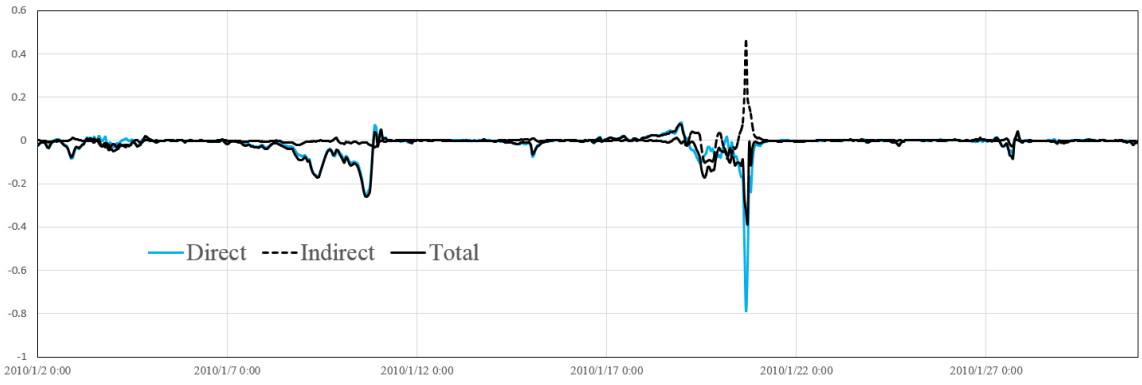

Figure 3.10 Time series of direct, indirect and total aerosol impacts on AOD550 during the haze event at BJ site

It can be seen from Figue 3.11 that the effect of indirect feedbacks on NRadF_TOA is relatively small except for an increase (up to 84 W/m^2) during the haze days. The effect of direct feedbacks is mostly negative at noon, except for an increase (up to 184 W/m^2) during the haze event.

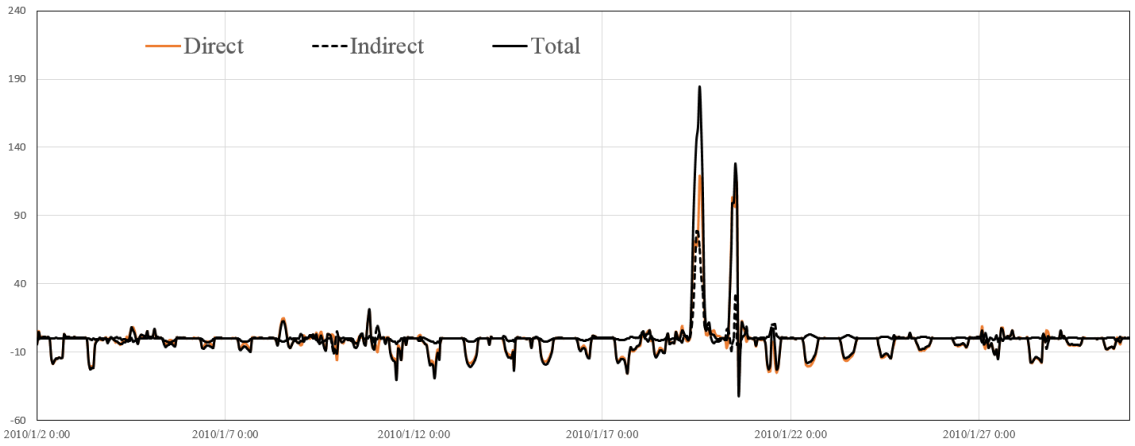

Figure 3.11 Time series of direct, indirect and total aerosol impacts on NRadF_AOD (W/m2) during the haze event at BJ site

The decreasing effect of direct feedbacks is even greater for NRadF_GRD (Figure 3.12). During the unpolluted days, the pattern of the time series is similar to that of NRadF_TOA except that the effect of direct feedbacks is greater. During the haze event, the direct feedbacks have a strong decreasing effect and the indirect feedbacks have an increasing effect.

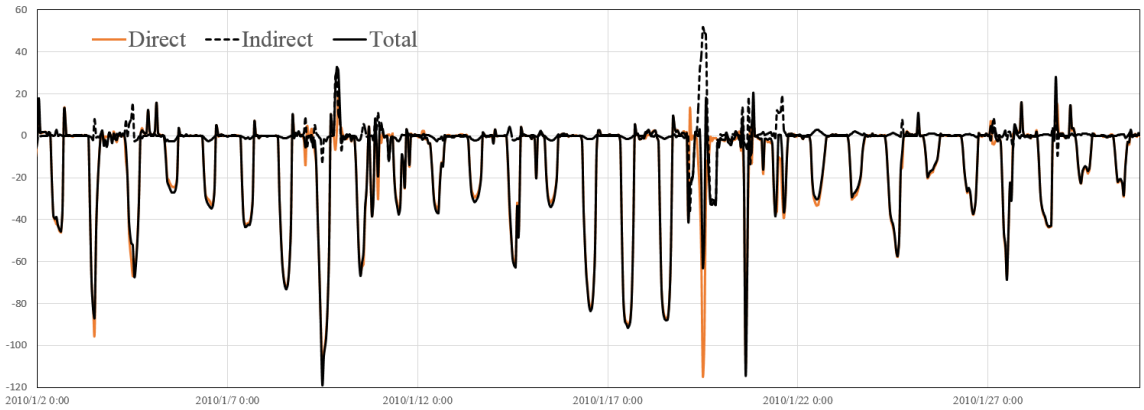

Figure 3.12 Time series of direct, indirect and total aerosol impacts on NRadF_GRD (W/m2) during the haze event at BJ site

The aerosol effects of NRadF_ATM are presented in Figure 3.13. The direct feedbacks have an increasing effect each day around noon, and the effect is greater during the haze days. The indirect feedbacks have a small increasing effect during the haze days, and does not show much effect on the rest of the days.

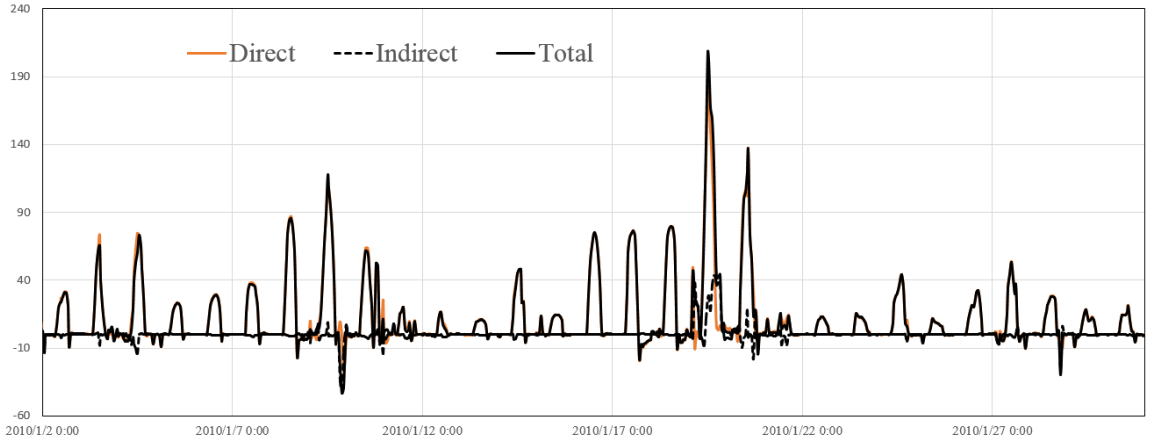

Figure 3.13 Time series of direct, indirect and total aerosol impacts on NRadF_ATM (W/m2) during the haze event at BJ site

3.3.2 Aerosol feedback impacts on surface $PM_{2.5}$ concentration during the haze

Similar to Section 3.4.1, the averaged effects of aerosol radiative feedbacks on $PM_{2.5}$ concentration during the haze event are calculated and presented in Figure 3.14. The direct feedbacks increased $PM_{2.5}$ up to over 16 $\mu m/m^3$ in Tianjin and south Hebei, and decreased $PM_{2.5}$ in the northwestern area in BTH. The indirect feedbacks, on the other hand, decreased $PM_{2.5}$ concentration in the same area. Overall, there are increases near Beijing and Tianjin, and the greatest increase located in south Hebei.

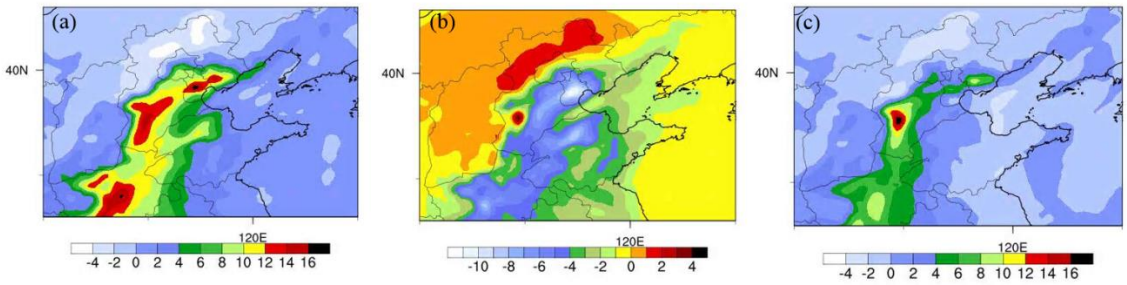

Figure 3.14 The spatial distribution of change in PM2.5 concentration (μm/m3) induced by (a) direct, (b) indirect and (c) both direct and indirect aerosol radiative feedback, averaged during Jan 16-21

The time series of aerosol feedback effects at Beijing Site are plotted and presented in Figure 3.15. The effect of indirect feedbacks is relatively weak in the clear days, and has a decreasing effect during the haze event, which can be as large as 40$\mu m/m^3$ at the end of the haze. The direct feedbacks helped the accumulation of $PM_{2.5}$ from the beginning of the haze event, and helped the dispersion of $PM_{2.5}$ in the end.

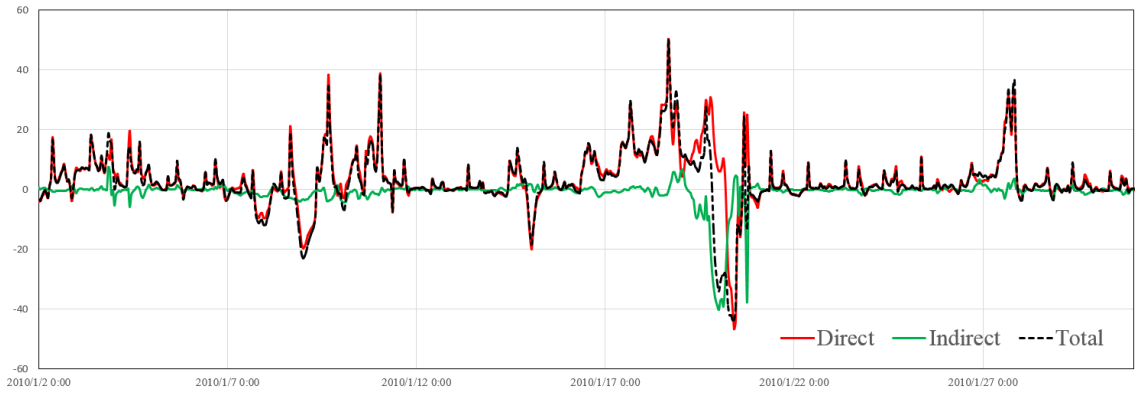

Figure 3.15 Time series of direct, indirect and total aerosol impacts on PM2.5 concentration (μm/m3) during the haze event at BJ site

Figure 3.16 shows the simulated and observed $PM_{2.5}$ concentration time series from January 12 to January 22. The red line represents the base scenario (without feedbacks) and the blue line represents the scenario with all feedbacks. It can be seen that from 12:00 to 17:00 on January 19, 2010, the $PM_{2.5}$ concentration of the simulation with all feedbacks is greater than the scenario without feedbacks. From the previous figures of time series, it can be seen that in the early afternoon of January 19, there was a cooler surface caused by a decrease in T2 and NRadF_GRD, as well as a warmer top of atmosphere caused by an increase in NRadF_TOA. In haze events, aerosol radiative feedbacks can increase temperature inversion and atmospheric stability, making the pollutants accumulate. On January 20, the wind speed increased more with the impact of aerosol radiative feedbacks, making the pollutants to disperse more easily.

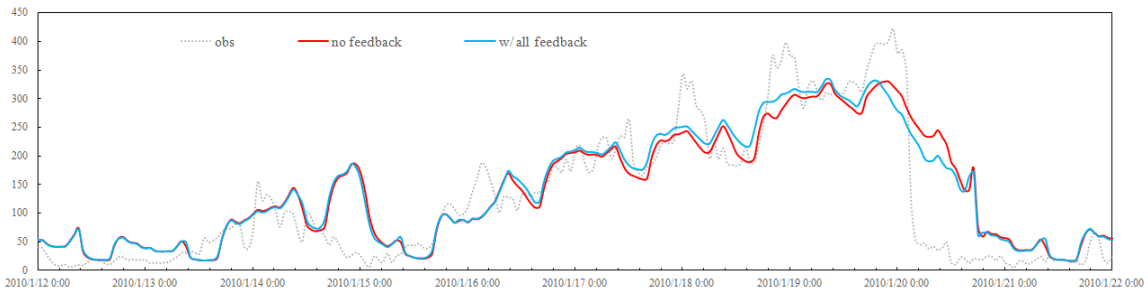

Figure 3.16 Time series of PM2.5 concentration (μm/m3) of the simulation scenarios with/without aerosol radiative feedbacks from January 12 to 22 at BJ site

3.3.3 Diurnal change of aerosol impacts on meteorological, radiative and pollutant variables

The averaged diurnal change of T2, Q2 and WS10 for January 16-21 are shown in Figure 3.17 (a) – (c). From the figures, the following conclusions can be drawn for the three variables:

1) The total feedbacks have a cooling effect for the whole day during the haze period. The indirect feedbacks have some warming effect from late morning to early afternoon.

2) The total feedbacks have a humidifying effect in almost any hour of a day during the haze period. The indirect feedbacks have some drying effect in the morning.

3) The total feedbacks from 09:00 to 18:00 can decrease WS10 by over 0.5 m/s, which created a stable meteorological condition and thus can help the accumulation of pollutants during the time period.

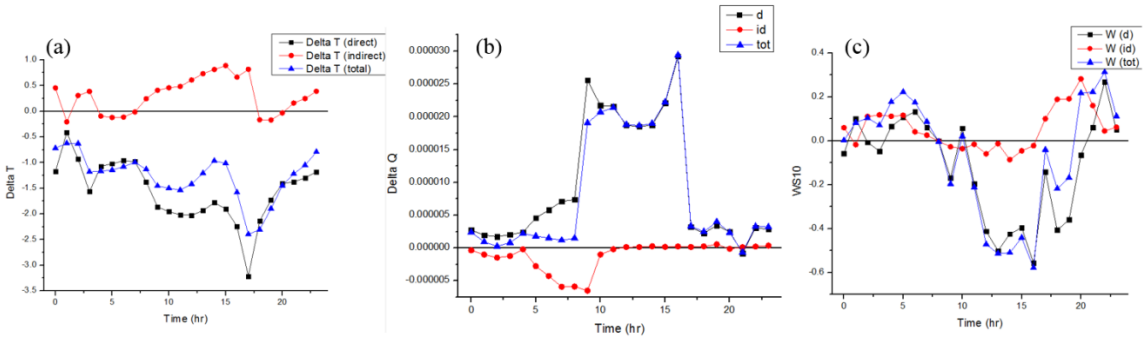

Figure 3.17 The hourly averaged changes of (a) T2 (°C), (b) Q2 (kg / kg) and (c) WS10 (m/s) induced by direct (black), indirect (red), and total (blue) aerosol radiative feedbacks at BJ site

Similarly, for the radiation variables, the averaged diurnal change of NRadF_TOA, NRadF_GRD and NRadF_ATM for January 16-21 are shown in Figure 3.18 (a) – (c). The following conclusions can be drawn:

1) At the top of atmosphere, both direct and indirect feedbacks increase the radiative forcing.

2) On the ground, although much radiation has been scattered, some radiation is stored in the atmosphere.

3) Most radiation left in the atmosphere is caused by the direct feedbacks.

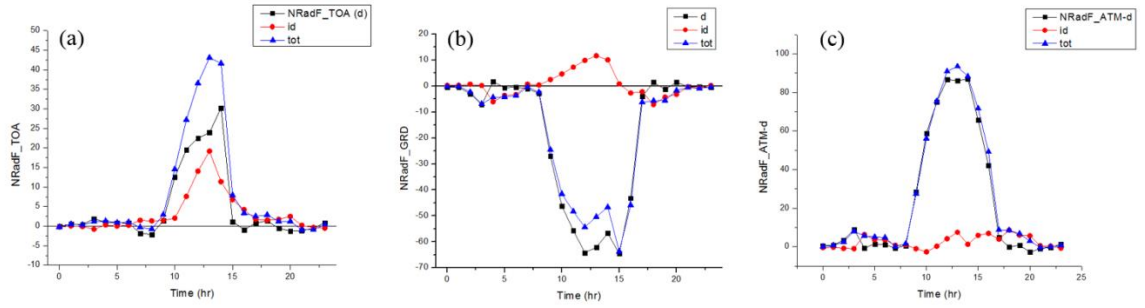

Figure 3.18 The hourly averaged changes of (a) NRadF_TOA (W/m2), (b) NRadF_GRD (W/m2) and (c) NRadF_ATM (W/m2) induced by direct (black), indirect (red), and total (blue) aerosol radiative feedbacks at BJ site

Figure 3.19 shows the diurnal change of aerosol effects on $PM_{2.5}$ concentration at BJ site during January 16-21. The total effect of radiation feedbacks is positive during the daytime, and is the most significant around 16:00 each day, and the smallest at 8:00. Figure 3.20 shows the hourly averaged $PM_{2.5}$ concentration at the same site during the same time period. It can be seen that the lowest hourly mean value of $PM_{2.5}$ concentration of each day occurs at around 15:00 and the highest value around 9:00. With the aerosol radiative effect, the high value of the concentration becomes smaller and the low value becomes larger, which weakens the diurnal variation. In the daytime, this phenomenon is mainly caused by direct feedbacks, and during the night it's mainly caused by indirect feedbacks.

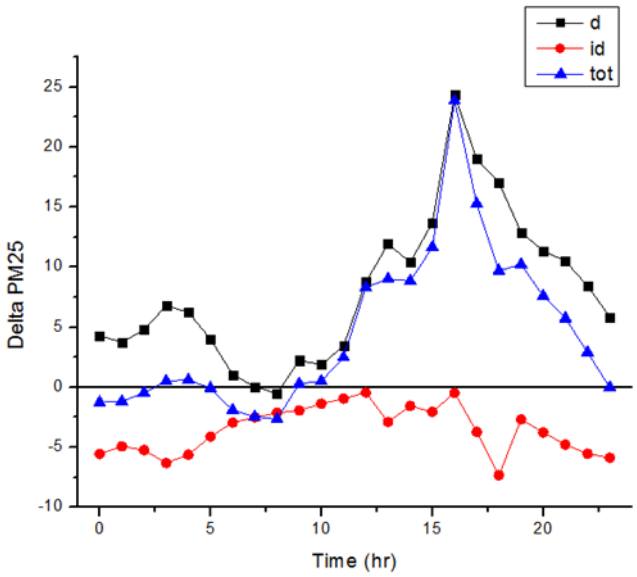

Figure 3.19 The hourly averaged changes of PM2.5 concentration (μm/m3) induced by direct (black), indirect (red), and total (blue) aerosol radiative feedbacks at BJ site

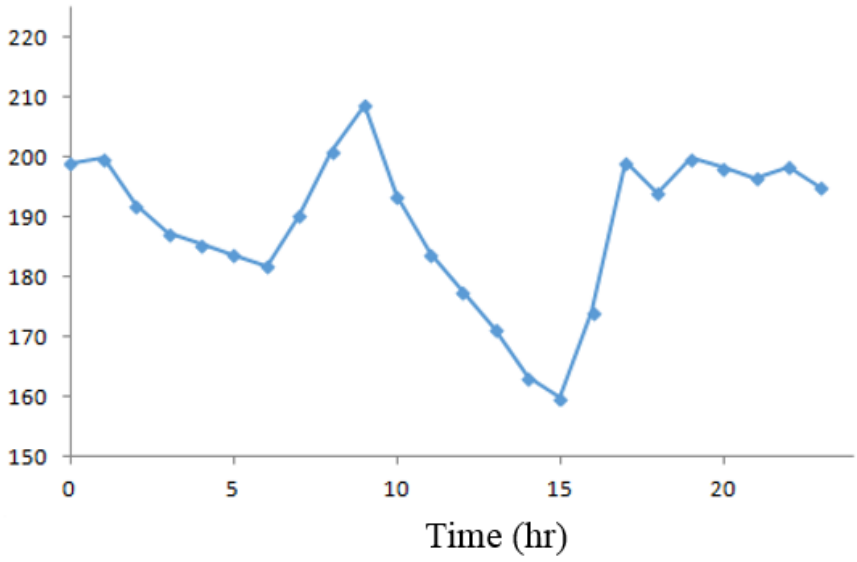

Figure 3.20 The hourly averaged PM2.5 concentration (μm/m3) during Januray 16-21 at BJ site

3.4 Summary

The direct and indirect feedbacks of aerosols have been evaluated in this chapter. The time series, spatial distributions and diurnal averages of the aerosol impact on meteorological, radiative and air pollutant variables have been analyzed. The severe haze period, January 16-21 has been taken a closer look at.

In BTH area during the haze event, the aerosol has a negative forcing of 1.4 °C in temperature, a negative forcing of 0.0001 to 0.0002 kg / kg in water vapor mixing ratio, a decrease of 0.01 to over 0.04 in AOD. The direct feedbacks play the dominant part of decreasing for these variables.

As for the radiative variables, both direct and indirect feedbacks have positive forcing at top of atmosphere, adding up to 20 W/m-2 in BTH area. The effect of total feedbacks on the ground is negative, with direct feedbacks having a greater negative

forcing and indirect feedbacks having a smaller positive forcing. The direct feedbacks play the dominant part as well.

The meteorological conditions become more stable because of the aerosol radiative feedback, and this situation makes it harder for pollutants to disperse. The PM2.5 concentration increased by up to more than 16μm/m3 in the southern part of the BTH area. At the peak of the haze pollution, PM2.5 concentration is increased by radiative feedbacks because of an increased atmospheric stability. Likewise, during the cleaning stage, PM2.5 concentration is decreased. The aerosol radiative forcing also causes a smaller diurnal variation of PM2.5 concentration.

CHAPTER 4 SUMMARY AND FUTURE WORK

This thesis focuses on a winter haze event in BTH region in January 2010. As a part of MICS-Asia III, evaluations of model simulations are made to get a better understanding of NU-WRF model.

The thesis first discussed the impact of horizontal resolution on the model performance. Results of model applications with two resolutions (45km and 15km, named D1 and D2 respectively) were compared. The performances for these two applications in urban and suburban sites have been examined as well.

In January 2010, simulations with both resolutions well estimate the meteorological variables except for an overestimation in wind speed for about 1m/s. Application with coarser resolution performs better in predicting the temperature at 2m. Hourly-averaged results show that simulation with a coarser resolution does not present obvious diurnal change of meteorology. The rapid change in the simulations for meteorological variables during the "cleaning" stage after the severe haze pollution shows a delay in the finer resolution simulation. The simulations of various air pollutants of both resolutions at urban and suburban sites are evaluated. The model performance is not very sensitive to the type of areas, but there has been some differences shown between and air pollutant species. Simulations of both resolutions can capture the overall trend of PM2.5 concentration, but fail to capture the daily peak of PM2.5 in urban/suburban site, and the PM2.5 concentration in the mountain site is overestimated.

The second object of this thesis is finding out the impact of direct and indirect aerosol radiative effect. The direct and indirect feedbacks of aerosols have been evaluated

in this chapter. The time series, spatial distributions and diurnal averages of the aerosol impact on meteorological, radiative and air pollutant variables have been analyzed.

The aerosol has a negative forcing in temperature, water vapor mixing ratio, and AOD. The direct feedbacks play the dominant role of decreasing for these variables. Both direct and indirect feedbacks have positive forcing at top of atmosphere. The effect of total feedbacks on the ground is negative, with direct feedbacks having a greater negative forcing and indirect feedbacks having a smaller positive forcing. The meteorological conditions become more stable because of the aerosol radiative feedback. This situation makes it harder for pollutants to disperse, so the PM2.5 concentration increased up to over 16 μm/m3 in the southern part of BTH area. The aerosol radiative forcing also causes a smaller diurnal variation of PM2.5 concentration.

In Chapter 2, the impact of resolutions on predictions of meteorology and air pollutants has been presented, and is more obviously shown in diurnal changes. The model is not very sensitive to the type of area (urban/suburban). In further researches, more detailed meteorology simulation and the emission activities in the area can be introduced to explain the performances between different sites. In Chapter 3, the contributions of different aerosol feedbacks are presented. In the future, the observed particle composition data in BTH can be introduced to find out the feedbacks of different particle species. Also, the results in this research may be used in the more detailed inter-comparison with other models in MICS-Asia III for a better understanding of CTMs.

REFERENCES

Boucher, O. et al 2013 Clouds and aerosols Climate Change 2013: The Physical Science Basis. Contribution of Working Group I to the Fifth Assessment Report of the Intergovernmental Panel on Climate Change ed T F Stocker, D Qin, G-K Plattner, M Tignor, S K Allen, J Boschung, A Nauels, Y Xia, V Bex and P M Midgley (Cambridge: Cambridge University Press)

Carmichael, G. R., Sakurai, T., Streets, D., Hozumi, Y., Ueda, H., Park, S. U., ... & Bennet, C. (2008). MICS-Asia II: The model intercomparison study for Asia Phase II methodology and overview of findings. Atmospheric Environment, 42(15), 3468-3490.

Charlson, R.J., Schwartz, S.E., Hales, J.M., Cess, R.D., Coakley Jr., J.A., Hansen, J.E., Hofmann, D.J., 1992. Climate forcing by anthropogenic aerosols. Science 255 (5043), 423-430.

Cheng, S., Yang, L., Zhou, X., Xue, L., Gao, X., Zhou, Y., and Wang, W.: Size-fractionated water-soluble ions, situ PH and water content in aerosol on hazy days and the influences on visibility impairment in Jinan, China, Atmos. Environ., 45, 4631–4640, 2011.

Chin, Mian, et al., 2002. Tropospheric aerosol optical thickness from the GOCART model and comparisons with satellite and sun photometer measurements. J. Atmos. Sci. 59, 461-483.

China, M.A., 2010. Observation and forecasting levels of haze.

Crippa, P., Sullivan, R. C., Thota, A., & Pryor, S. C. (2017). The impact of resolution on meteorological, chemical and aerosol properties in regional simulations with WRF-Chem. Atmospheric Chemistry and Physics, 17(2), 1511.

Gao, M., Carmichael, G. R., Wang, Y., Saide, P. E., Yu, M., Xin, J., ... & Wang, Z. (2016). Modeling study of the 2010 regional haze event in the North China Plain. Atmos. Chem. Phys, 16(3), 1673-1691.

Gao, M., Guttikunda, S.K., Carmichael, G.R., Wang, Y., Liu, Z., Stanier, C.O., Saide, P.E., Yu, M., 2015b. Health impacts and economic losses assessment of the 2013 severe haze event in Beijing area. Sci. Total Environ. 511, 553–561.

Gao, M., Han, Z., Liu, Z., Li, M., Xin, J., Tao, Z., Li, J., Kang, J.-E., Huang, K., Dong, X., Zhuang, B., Li, S., Ge, B., Wu, Q., Cheng, Y., Wang, Y., Lee, H.-J., Kim, C.-H., Fu, J. S., Wang, T., Chin, M., Woo, J.-H., Zhang, Q., Wang, Z., and Carmichael, G. R.: Air Quality and Climate Change, Topic 3 of the Model Inter-Comparison Study for Asia Phase III (MICS-Asia III), Part I: overview and model evaluation, Atmos. Chem. Phys. Discuss., doi:10.5194/acp-2017-731, in review, 2017.

Grell, G., Freitas, S.R., Stuefer, M., Fast, J., 2011. Inclusion of biomass burning in WRFChem: impact of wildfires on weather forecasts. Atmospheric Chemistry and Physics 11, 5289-5303.

Kuik, F., Lauer, A., Churkina, G., van der Gon, H. A. D., Fenner, D., Mar, K. A., & Butler, T. M. (2016). Air quality modelling in the Berlin-Brandenburg region using WRF-Chem v3. 7.1: sensitivity to resolution of model grid and input data. Geoscientific Model Development, 9(12), 4339.

Lelieveld, J., Evans, J. S., Fnais, M., Giannadaki, D., & Pozzer, A. (2015). The contribution of outdoor air pollution sources to premature mortality on a global scale. Nature, 525(7569), 367-371.

Li, M., Zhang, Q., Kurokawa, J., Woo, J. H., He, K. B., Lu, Z., ... & Cheng, Y. F. (2015). MIX: a mosaic Asian anthropogenic emission inventory for the MICS-Asia and the HTAP projects. Atmos. Chem. Phys. Discuss, 15(23), 34-813.

Li, Z., Gu, X., Wang, L., Li, D., Xie, Y., Li, K., Dubovik, O., Schuster, G., Goloub, P., Zhang, Y., Li, L., Ma, Y. and Xu, H.: Aerosol physical and chemical properties retrieved from ground-based remote sensing measurements during heavy haze days in Beijing winter, Atmos. Chem. Phys., 13(20), 10171–10183

Nishikawa, Y., & Kannari, A. (2011). Atmospheric concentration of ammonia, nitrogen dioxide, nitric acid, and sulfur dioxide by passive method within Osaka prefecture and their emission inventory. Water, Air, & Soil Pollution, 215(1-4), 229-237.

Peters-Lidard, C.D., Houser, P.R., Tian, Y., Kumar, S.V., Geiger, J., Olden, S., Lighty, L.,Doty, B., Dirmeyer, P., Adams, J., Mitchell, K., Wood, E.F., Sheffield, J., 2007. Highperformance earth system modeling with NASA/GSFC's land information System. Innov. Syst. Softw. Eng. 3 (3), 157-165.

Quan, J., Zhang, Q., He, H., Liu, J., Huang, M., and Jin, H.: Analysis of the formation of fog and haze in North China Plain (NCP), Atmos. Chem. Phys., 11, 8205–8214

Streets, D. G., Bond, T. C., Carmichael, G. R., Fernandes, S. D., Fu, Q., He, D., ... & Woo, J. H. (2003). An inventory of gaseous and primary aerosol emissions in Asia in the year 2000. Journal of Geophysical Research: Atmospheres, 108(D21).

Tan, J., Zhang, Y., Ma, W., Yu, Q., Wang, J., & Chen, L. (2015). Impact of spatial resolution on air quality simulation: A case study in a highly industrialized area in Shanghai, China. Atmospheric Pollution Research, 6(2), 322-333.

Tie, X., Brasseur, G., & Ying, Z. (2010). Impact of model resolution on chemical ozone formation in Mexico City: application of the WRF-Chem model. Atmospheric Chemistry and Physics, 10(18), 8983-8995.

Twomey, S., 1974. Pollution and the planetary albedo. Atmospheric Environment 8, 1251-1256

Van Donkelaar, A., Martin, R. V., Brauer, M., Kahn, R., Levy, R., Verduzco, C., Villeneuve, P.J., 2010. Global estimates of ambient fine particulate matter concentrations from satellitebased aerosol optical depth: Development and application. Environ. Health Perspect. 118, 847–855

Wang, Z., Li, J., Wang, Z., Yang, W., Tang, X., Ge, B., Yan, P., Zhu, L., Chen, X., Chen, H., Wand, W., Li, J., Liu, B., Wang, X., Zhao, Y., Lu, N. and Su, D.: Modeling study of regional severe hazes over mid-eastern China in January 2013 and its implications on pollution prevention and control, Sci. China Earth Sci., 57(1), 3–13, doi:10.1007/s11430- 013-4793-0, 2014e.

Xin, J., Wang, Y., Pan, Y., Ji, D., Liu, Z., Wen, T., ... & Wang, P. (2015). The campaign on atmospheric aerosol research network of China: CARE-China. Bulletin of the American Meteorological Society, 96(7), 1137-1155.

Yu, X., Zhu, B., Yin, Y., Yang, J., Li, Y. and Bu, X.: A comparative analysis of aerosol properties in dust and haze-fog days in a Chinese urban region, Atmos. Res., 99(2), 241– 247, doi:10.1016/j.atmosres.2010.10.015, 2011.

Zhang, Q., Streets, D. G., Carmichael, G. R., He, K. B., Huo, H., Kannari, A., Klimont, Z., Park, I. S., Reddy, S., Fu, J. S., Chen, D., Duan, L., Lei, Y., Wang, L. T., and Yao, Z. L.: Asian emissions in 2006 for the NASA INTEX-B mission, Atmos. Chem. Phys., 9, 5131–5153

Zhang Y 2008 Online-coupled meteorology and chemistry models: history, current status, and outlook Atmos. Chem. Phys. 8 1833–912

Zhao, C., Liu, X., Leung, L. R., Johnson, B., McFarlane, S. A., Gustafson Jr., W. I., Fast, J. D., and Easter, R.: The spatial distribution of mineral dust and its shortwave radiative forcing over North Africa: modeling sensitivities to dust emissions and aerosol size treatments, Atmos. Chem. Phys., 10, 8821–8838